NANO MICRO small

Supporting Information

for *Small*, DOI: 10.1002/smll.201200139

Graphene Enhances the Specificity of the Polymerase Chain Reaction

Jing Jia, Liping Sun, Nan Hu, Guoming Huang, and Jian Weng**

Submitted to small NANO MICRO

Supporting Information should be included here (for submission only; for **publication**, please provide Supporting Information as a separate PDF file).

Supporting Information

Graphene Enhances the Specificity of Polymerase Chain Reaction

Jing Jia, Liping Sun, Nan Hu, Guoming Huang and Jian Weng**

Department of Biomaterials, College of Materials, Xiamen University, Xiamen 361005 (P.R. China)

E-mail: sunliping@xmu.edu.cn; jweng@xmu.edu.cn

1. Preparation and characterizeation of chemical reduced graphene oxide

Graphite oxide was synthesized from graphite through the modified Hummers method.[1, 2] As-synthesized graphite oxide was suspended in water to give a brown dispersion, which was subjected to dialysis for completely removing residual salts and acids. The purified graphite oxide was then dispersed in water to make a 0.1 mg mL^{-1} suspension. Exfoliation of graphite oxide to graphene oxide (GO) was achieved by ultrasonication of the dispersion using a Kudos Sonifier (SK8210HP, 500W) for 30 min. Chemical reduced graphene oxide (RGO) was prepared in ammonia with hydrazine hydrate as a reducing agent.[3] The excess ammonia in the resulting RGO solution was removed by dialysis for a week. The product was centrifuged and washed with deionized water several times. The resulting RGO was dried at 60 °C in a vacuum overnight. 10 mg of RGO power was dispersed in 100 mL of water with

ultrasonic treatment to produce a final concentration of 0.1 mg mL^{-1} for the PCR reactions. Before it was used, the dispersion was exposed to UV light for about 30 min to avoid DNase and RNase contamination. Then the suspension was ultrasonicated for about 30 min to maintain the stability and dispersibility.

X-ray photoelectron spectroscopy (XPS) spectra were recorded on a PHI QUANTUM 2000 XPS. The crystallographic structures of the materials were determined by a powder X-ray diffraction system (XRD, Philips PANAlytical X'pert) equipped with Cu Kα radiation (λ=0.1541 nm). UV-vis spectroscopy spectra were collected on a Beckman H800 spectrophotometer with 1 nm resolution. The Fourier transform infrared (FTIR) spectrum of the sample was recorded on a Nicolet AVATR 360 FTIR spectrometer at room temperature. The atomic force microscopy (AFM) images were taken in tapping mode with an Agilent 5500 AFM.

2. Characterization of the GO and RGO

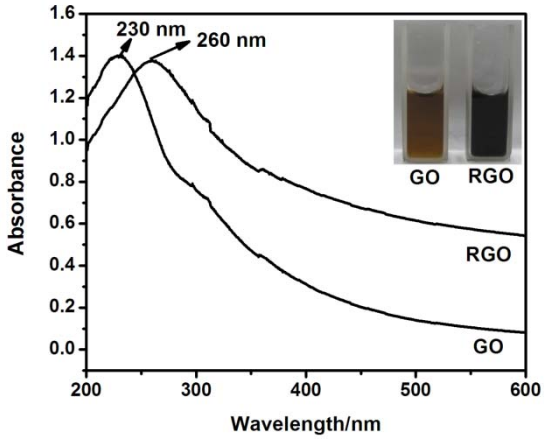

Figure S1. UV-vis spectra of GO and RGO suspension. Inset: photographs of GO and RGO.

Figure S1 shows The UV-vis absorption spectra of GO and RGO solution. The GO dispersion displays a maximum absorption at 230 nm which is due to the π-π* transition of aromatic C=C bonds and a shoulder at 290-300 nm which corresponds to the n-π* transition of the C=O bond.[4] As the reduction reaction proceeds, the characterized absorption peak

(230 nm) gradually red-shifts to 260 nm indicating the electronic conjugation within the graphene sheets is restored. The inset shows the color change of 0.5 mg mL^{-1} GO solution from yellow brown to black after reduction.

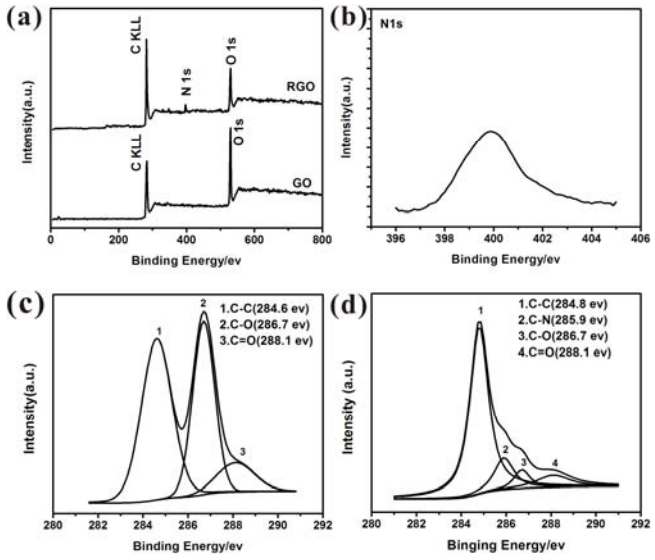

Figure S2. XPS spectra of GO and RGO (a), N1s spectrum of RGO (b), C1s spectra of GO (c) and RGO (d).

.

X-ray photoelectron spectroscopic (XPS) data (Figure S2) provided further information for the GO-to-RGO conversion. The XPS spectrum (Figure S2a) of RGO shows evident existence of N1s compared to the spectrum of GO. Figure S2b displays the N1s spectrum of RGO. The deconvolution of C1s spectrum of GO in Figure S2c indicates the GO is consisted by the following functional groups: C-O (epoxy/ hydroxyl, 286.7 eV), C=O (carbonyl, 288.1 eV), and C-C (284.6 eV). Figure S2d is a C1s spectrum of RGO. The additional component at 285.9 eV is assigned to the C-N bond which results from the bond formation by hydrazine.[5] The reduction effect is clear since the content of all oxygen-containing functional groups of RGO significantly decreased yet the peak intensity of C-C increased.

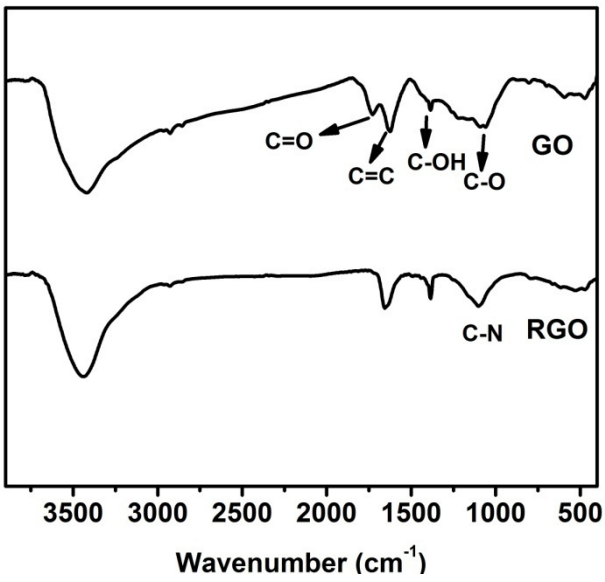

Figure S3. FT-IR spectra of GO and RGO.

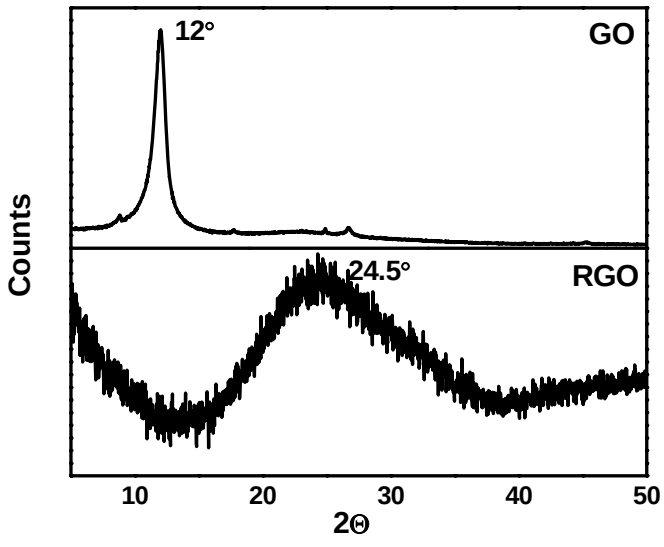

Figure S4. X-ray diffraction patterns of GO and RGO.

Figure S4 exhibits the XRD patterns which supports the same order of overall oxidation. For XRD, the interlayer spacing of the material is proportional to the degree of oxidation. The feature diffraction peak of GO appears at 12° indicates the layer-to-layer distance is 7.4 Å. Also, the peak at 26.7° shows the presence of pristine graphene with d-spacing of 3.4 Å contributing to the intercalated water molecules between layers.[6,7] After reduction, the sharp peak at 12° disappears yet shows a broad peak at 24.5° corresponding to the 3.7 Å of d-spacing. The width of the RGO peak in the XRD pattern can be attributed to two factors: first, the small sheet size (1 μm and below), second, a relatively short domain order or turbostratic arrangement of RGO stacked sheets, each of which broadens the XRD peak.[8]

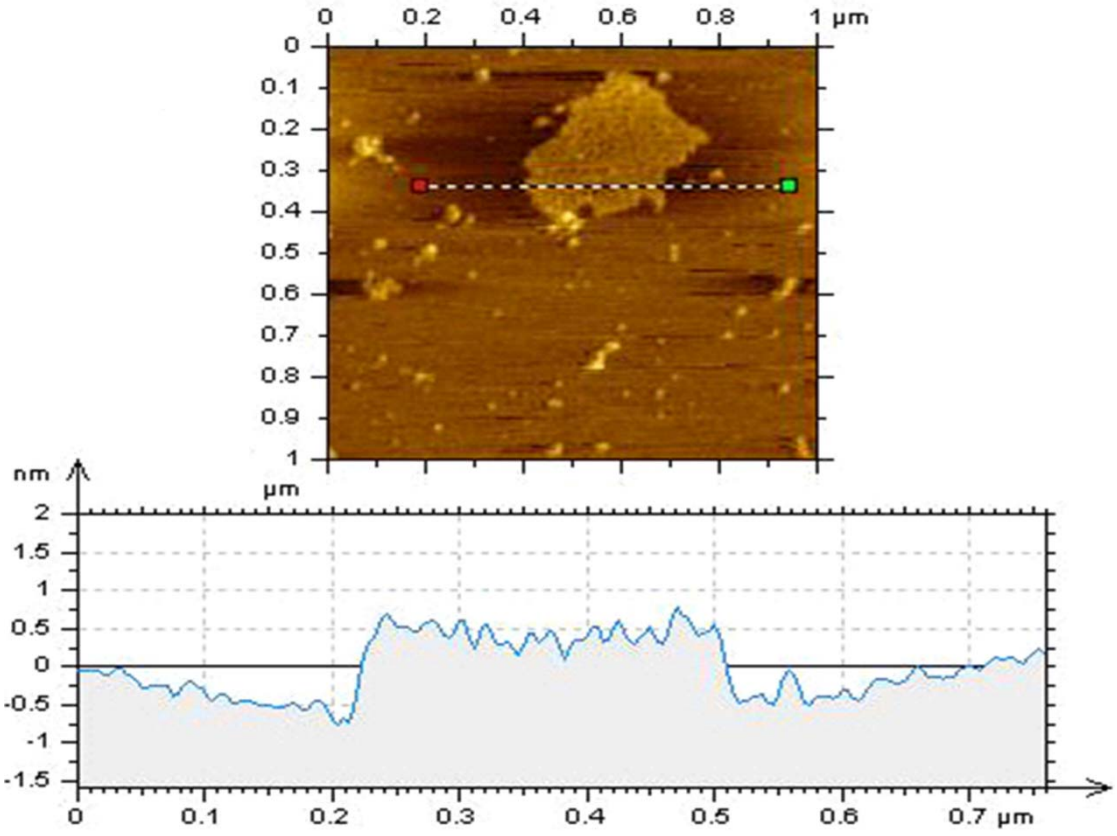

Figure S5. AFM images of RGO with a height profile.

```
Seq 1 TTATGAAACTTAAGGGTCGAAGGTGGATTTAGCAGTAAACTAAGAGTAGAGTGCTTAGTTGAACA 65
Seq 2 TTATGAAACTTAAGGGTCGAAGGTGGATTTAGCAGTAAACTAAGAGTAGAGTGCTTAGTTGAACA 65

Seq 1 GGGCCCTGAAGCGCGTACACACCGCCCGTCACCCTCCTCAAGTATACTTCAAAGGACATTTAAC 129
Seq 2 GGGCCCTGAAGCGCGTACACACCGCCCGTCACCCTCCTCAAGTATACTTCAAAGGACATTTAAC 129

Seq 1 TAAAACCCCTACGCATTTATATAGAGGAGACAAGTCGTAACATGGTAAGTGTACTGGAAAGTGC 193
Seq 2 TAAAACCCCTACGCATTTATATAGAGGAGACAAGTCGTAACATGGTAAGTGTACTGGAAAGTGC 193

Seq 1 ACTTGGACGAACCAGAGTGTAGCTTAACACAAAGCACCCAACTTACACTTAGGAGATTTCAACT 257
Seq 2 ACTTGGACGAACCAGAGTGTAGCTTAACACAAAGCACCCAACTTACACTTAGGAGATTTCAACT 257

Seq 1 TAACTTGACCGCTCTGAGCTAAACCTAGCCCCAAACCCACTCCACCTTACTACCAGACAACCTTA 322
Seq 2 TAACTTGACCGCTCTGAGCTAAACCTAGCCCCAAACCCACTCCACCTTACTACCAGACAACCTTA 322

Seq 1 GCCAAACCATTTACCCAAATAAAGTATAGGCGATAGAAATTGAAACCTGGCGCAATAGATATAGT 387
Seq 2 GCCAAACCATTTACCCAAATAAAGTATAGGCGATAGAAATTGAAACCTGGCGCAATAGATATAGT 387

Seq 1 ACCGCAAGGGAAAGATGAAAAATTATAACCAAGCATAATATAGCAAGGACTAACCCCTATACCTT 452
Seq 2 ACCGCAAGGGAAAGATGAAAAATTATAACCAAGCATAATATAGCAAGGACTAACCCCTATACCTT 452

Seq 1 CTGCATAATGAATTAACTAGAAATAACTTTGCAAGGAGAGCCAAAGCTAAGACCCCCGAAACCA 516
Seq 2 CTGCATAATGAATTAACTAGAAATAACTTTGCAAGGAGAGCCAAAGCTAAGACCCCCGAAACCA 516

Seq 1 GACGAGCTACCTAAGAACAGCTAAAAGAGCACACCCGTCTATGTAGCAAAATAGTGGGAAGATT 580
Seq 2 GACGAGCTACCTAAGAACAGCTAAAAGAGCACACCCGTCTATGTAGCAAAATAGTGGGAAGATT 580

Seq 1 TATAGGTAGAGGCGACAAACCTACCGAGCCTGGTGATAGCTGGTTGTCCAAGATAGAATCTTAG 644
Seq 2 TATAGGTAGAGGCGACAAACCTACCGAGCCTGGTGATAGCTGGTTGTCCAAGATAGAATCTTAG 644

Seq 1 TTCAACTTTAAATTTGCCCACAGAACCCTCTAAATCCCC- -TTGTAAATTTAACTGTTAGTCCAAA 710
Seq 2 TTCAACTTTAAATTTGCCCACAGAACCCTCTAAATCCCTCATTGTAAATTTAACTGTTAGTCCTAC 710

Seq 1 GAG - - -GAACAGCTCTT 727
Seq 2 AAGAGTGAACAGCTCTT 727
```

Figure S6. Sequencing results of the amplification fidelity of RGO-assisted PCR. Forward and reverse primers were used for sequencing and the sequence read from reverse primer was converted to a sense strand sequence and compared with the sequence read from forward primer. Seq 1: without RGO; Seq 2: with RGO.

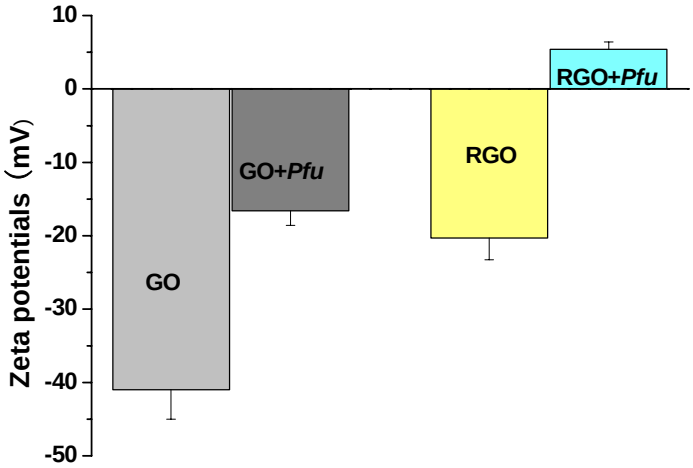

Figure S7. Zeta potentials of GO and RGO solutions. Data are the mean ± standard deviation of three different experiments with 10% relative standard deviation.

References：

[1] N. I. Kovtyukhova, P. J. Ollivier, B. R. Martin, T. E. Mallouk, S. A. Chizhik, E. V. Buzaneva, A. D. Gorchinskiy, *Chem. Matter.* **1999**, *11*, 771.

[2] W. S. Hummers, R. E. Offeman, *J. Am. Chem. Soc.* **1958**, *80*, 1339.

[3] D. Li, M. B. Müller, S. Gilje, R. B. Kaner, G. G. Wallace, *Nature Nanotechnol.* **2008**, *03*, 101.

[4] Y. J. Guo, L. Deng, S. J. Guo, E. K. Wang, S. J. Dong, *ACS Nano* **2011**, *5*, 1285.

[5] S. Dubin, S. Giije, K. Wang, V. C. Tung, K. Cha, A. S. Hall, J. Farrar, R. Varshneya, Y. Yang, R. B. Kaner, *ACS Nano* **2010**, *04*, 3845.

[6] H. L. Guo, X. F. Wang, Q. Y. Qian, F. B. Wang, X. H. Xia, *ACS Nano* **2009**, *03*, 2653.

[7] D. C. Marcano, D. V. Kosynkin, J. M. Berlin, A. Sinitskii, Z. Z. Sun, A. Slesarev, L.B. Alemany, W. Lu, J. M. Tour, *ACS Nano* **2010**, *04*, 4806.

[8] S. Dubin, S. Giije, K. Wang, V. C. Tung, K. Cha, A. S. Hall, J. Farrar, R. Varshneya, Y. Yang, R. B. Kaner, *ACS Nano* **2010**, *04*, 3845.